



Open Archive TOULOUSE Archive Ouverte (OATAO)

OATAO is an open access repository that collects the work of Toulouse researchers and makes it freely available over the web where possible.

This is an author-deposited version published in : <http://oatao.univ-toulouse.fr/>
Eprints ID : 11014

To link to this article : doi:10.1039/C3EE44114H
URL : <http://dx.doi.org/10.1039/C3EE44114H>

To cite this version : Ketep, Stephanie F. and Bergel, Alain and Calmet, Amandine and Erable, Benjamin Stainless steel foam increases the current produced by microbial bioanodes in bioelectrochemical systems. (2014) Energy & Environmental Science, vol. 6 (n° 5). pp. 1633-1637. ISSN 1754-5692

Any correspondence concerning this service should be sent to the repository administrator: staff-oatao@listes-diff.inp-toulouse.fr

Stainless steel foam pushes the current provided by microbial bioanodes for bioelectrochemical systems

Stéphanie F. Ketep*, Alain Bergel, Amandine Calmet, and Benjamin Erable

Stainless steel is raising increasing interest as an anodic material in bioelectrochemical systems and beginning to challenge the more conventional carbon-based materials. Here, microbial bioanodes designed in optimal conditions on carbon cloths gave high current densities, 33.5 +4.5 A/m² at -0.2 V/SCE, which were largely outstripped by the 60 to 80 A/m² at the same potential and more than 100 A/m² at 0.0 V/SCE provided by stainless steel foams.

Introduction

The exceedingly large majority of microbial bioanodes has been developed on graphite or carbon-based materials so far. However, stainless steel (SS) meshes are often contemplated as current collectors to overcome the insufficient electronic conductivity of carbon materials when the objective is to develop large-size bioanodes. An elegant solution to scale-up bioanodes would thus consist in growing directly the electroactive biofilm on stainless steel. Nevertheless, studies in this direction remain very rare.

Pioneering work¹ in 2008 demonstrated the suitability of SS as electrode material for both bioanodes and biocathodes in a prototype marine microbial fuel cell. Nevertheless, electron transfer appeared to be limited by the semiconducting properties of the SS passive layer at potentials higher than -0.15 V/SCE². Consequently, SS has been mainly employed for cathodes, because they operate at potentials lower than -0.15 V/SCE. Efficient biocathodes have thus been designed either with pure cultures²⁻⁴ or wild inocula^{5,6} and with various electrode morphologies including plates^{3,7} and mesh^{8,9}.

Since 2008, SS bioanodes have been investigated only sporadically. They have been implemented at low applied potential in order to avoid the semiconducting behaviour of oxide layers. Efficient microbial bioanodes providing up to 4 A/m² were thus obtained on plain SS with a natural biofilm scraped from harbour equipment, and 8.2 A/m² was then reached by replacing the plate electrode by a grid⁶. Recently, SS bioanodes have given the highest current densities reported so far with plain electrodes¹⁰. Current densities as high as 20.6 A/m² were obtained at -0.2

V/SCE, while it is generally agreed that microbial bioanodes developed on plain graphite do not exceed 10 to 15 A/m²¹¹.

Up to now, no three-dimensional SS structures have been tested, although there is a considerable amount of detailed literature on 3-D carbon materials: felt, brush, foam...¹². Only a few attempts at macro- or micro-structuring of SS surface have been reported, with limited increases in the current density¹⁰.

The objective of the present work was to check whether it was possible to increase the current density generated by SS bioanodes by using SS foams, similarly to what has been described with 3D carbon electrodes^{13,14}. High porosity SS foam was used and the performance was compared with that of microbial bioanodes formed on carbon cloth in identical conditions, which were used as a well-mastered positive control.

Results and discussion

Stainless steel foam compared to carbon cloth

Two bioanodes were developed in parallel with the same inoculum in two different reactors, under constant polarization at -0.2 V/SCE, with successive additions of 20 mM sodium acetate (Figure 1). One reactor was equipped with a carbon cloth anode, the other with a SS foam one, each having a projected surface area of 2 cm².

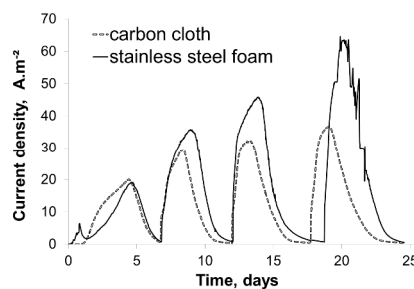


Fig. 1: Variation of current density with time for carbon cloth and stainless steel foam bioanodes polarized at -0.2 V/SCE.

Both electrodes gave similar current evolution over time. The maximum current density generated by the carbon cloth bioanode showed no significant increase from the second acetate addition onwards. Two acetate additions were sufficient for the electroactive biofilm to reach a stable maximum current. In contrast, the maximum current produced by the SS foam bioanode increased continuously over four successive acetate additions, up to a current density considerably higher than those provided by the carbon cloth bioanode. Two other experimental runs were performed, each using three reactors equipped either with carbon cloth anodes or with SS foam anodes. The results confirmed the initial observations (Figure 2). The four carbon cloth bioanodes produced current densities ranging from 29 to 38 A/m², while 63 to 82 A/m² were reached with SS foams.

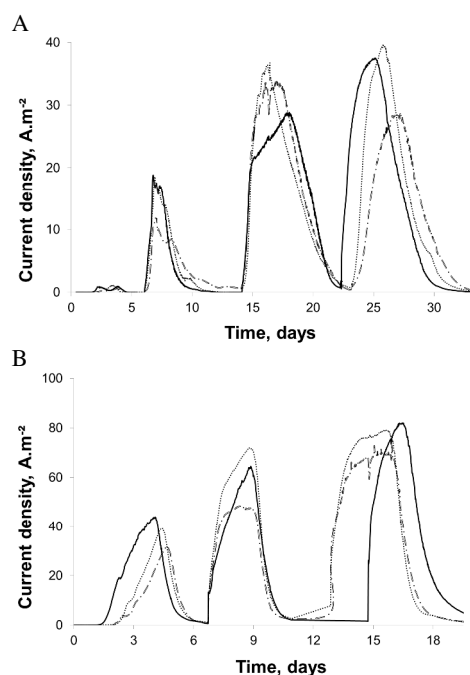


Fig. 2: Three bioanodes developed in parallel in independent reactors under polarization at -0.2 V/SCE on (A) carbon cloth electrodes and (B) stainless steel foams.

The discrepancies that can be seen between the two experimental runs, particularly during the early formation phases, were induced by the nature of inoculum. Reactors were filled with compost leachate that constituted both the inoculum and the medium, without any supplementation other than KCl (when preparing the leachate) and sodium acetate. It was consequently difficult to control the microbial and chemical compositions of the solution and differences could occur from one experimental run to another. Such experimental variations have already been observed and commented in studies implementing wild inocula in wild solutions^{15,16}. Nevertheless, here, the differences between carbon cloths and SS foams were large enough to allow their difference in performance to be clearly observed despite the experimental variations.

Discussion / positioning on the performance

The maximum current densities of 33.5 ± 4.5 A/m² obtained here

at -0.2 V/SCE with carbon cloth anodes were of the same order of magnitude as those already reported under the same experimental conditions¹⁰. These values are among the highest current densities reported for microbial bioanodes so far, except for experiments implementing multi-layered electrode architecture¹⁷. Carbon foams have been prepared by direct carbonization of natural products, kenaf stems (plant)¹³ or pomelo peel (fruit)¹⁴, to form the support for bioanodes. Current densities of 32.5 and 40 A/m² respectively have been obtained at +0.2 V/Ag/AgCl. The value of 40 A/m² was 5 times that provided by commercial reticulated vitreous carbon foam (8.1 A/m²) and 2.5 times that with graphite felts (17.9 A/m²) in identical experimental conditions. Sponges have also been employed as anode supports after coating their surface with nickel¹⁸ or carbon nanotubes¹⁹, and led to power and current densities of 996 mW/m² and 21.3 A/m² at 0.15 V vs. Ag/AgCl, respectively. Basically, an anode must provide the highest possible current density at the lowest possible potential. It is consequently essential to compare current densities at the same potential. According to the voltammetry curves reported, the best performing kenaf stems and pomelo peel foams provided only around 18 A/m² at the potential of -0.2 V/ECS used in the present work (or -0.245 V vs. Ag/AgCl). In terms of current density, carbon foam bioanodes have consequently had limited success so far, in comparison with some 2-dimensional electrodes such as carbon cloth.

In contrast, SS foams considerably improved the performance of stainless steel. The highest current densities reported for bioanodes developed on SS plates were 21 A/m²¹⁰, while 63 to 82 A/m² were reached here with SS foams. These values of current density should be qualified as they were calculated with respect to the projected surface area (2 cm²). Nevertheless, exactly the same set-ups and calculations were used for the SS plates used in the previous work and the carbon cloth and SS foam used here. The comparison in high favour of SS foam was consequently fully relevant.

Biofilms structures on carbon cloth and SS foam

SEM observation of the clean carbon cloth and SS foam showed very different structures (Fig. 3). The carbon cloth (fibres 10 μm in diameter) had a very tight network of interwoven 300-μm threads (Fig. 3A). It had a large developed surface area, which multiplied the probability of adhesion of microorganisms in the early stage of biofilm formation and contributed to its good electrochemical performance. Nevertheless, the bioanode obtained after 25 days of polarization (Fig. 3C) showed a thick, uniform biofilm, which covered the entire electrode surface and masked the morphology of the cloth. The external biofilm topography was similar to that which could be obtained on a plain surface. The surface of the electrode was smoothed by the biofilm. Similar observations have been reported in the literature. A fully developed wild biofilm has been shown to mask the micrometre-sized roughness of the electrode surface¹¹. Zhang et al.²⁰ showed that coating the electrode surface with carbon nanotubes enhanced the initial phase of biofilm growth, but no longer increased the bioanode performance after complete

development of the biofilm. The chaotic topography of the carbon cloth used here certainly contributed to the development of a dense carpet of electroactive bacteria on its surface but it did not increase the surface area of the biofilm exposed to the solution.

In contrast, the SS foam presented an open structure with cylindrical pores having diameters between 200 and 800 μm (figure 3B). A large cross sectional area was available for the microorganisms to penetrate into the 3D structure and exploit a large part of the internal surface area of the electrode. The biofilm grown on SS foam (figure 3D) presented the expected structure, penetrating the internal volume of the foam and not clogging the pores. Its thickness was measured at around 20 μm , while the diameters of the electrode pores were 10 to 40 times larger.

Bioanodes were developed in parallel on SS foams with or without stirring of the solution. Under stirring, the bioanodes started to produce current after only 6 hours, while 24 hours were necessary without stirring. Stable maximum currents were also obtained faster under stirring, in only one week. Stirring increased the probability of microorganisms contacting the electrode surface and also enhanced penetration of the microorganisms into the 3D structure. The rate of bioanode stabilization was thus shorter under stirring. However, no difference was observed in the final maximum current densities, which were of the same order of magnitude (75 to 80 A/m^2) with or without stirring. The effect of stirring on bioanode formation showed that the transport of microorganisms into the electrode structure was a rate-limiting step during biofilm development. In contrast, the absence of an effect of stirring on the maximum currents obtained indicated that mass transfer of the substrate and products was not rate-limiting for the electrochemical process.

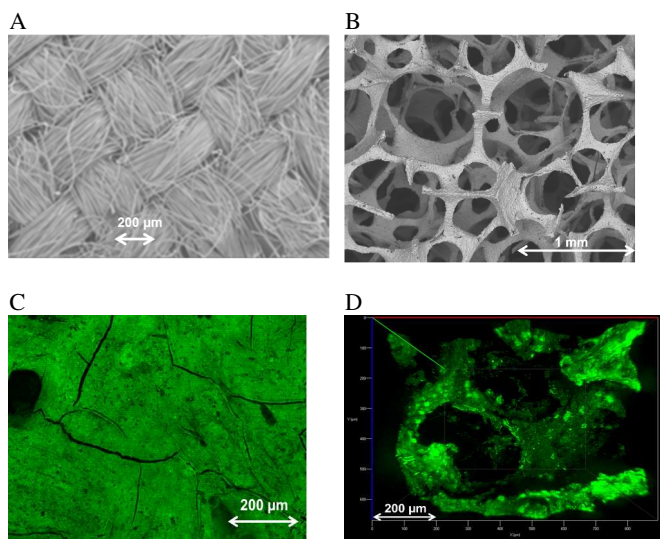


Fig. 3: SEM images of clean electrodes: (A) carbon cloth, (B) SS foam; and 3D epifluorescent microscopy of bioanodes formed under polarization at $-0.2 \text{ V}/\text{ECS}$ on (C) carbon cloth, (D) SS foam.

High porosity and large pore sizes, which allowed the biofilm to develop inside the foam and did not hinder mass transfer, are the pillars of the high performance obtained here. The global porosity is an important parameter, but pore size is also essential. For

example, pore sizes in the micrometre range have been shown to be detrimental to long-term application of a carbon fibre electrode because of pore clogging, despite its porosity of 99%¹¹. Carbon foam electrodes derived from kenaf stem with pore sizes in the 20-60 μm range have also shown transport limitation due to cell valves¹³. In contrast, the best-performing carbon foam reported in the literature combined high porosity (98%) and large pore size (300-500 μm)¹⁴.

Cyclic voltammetry

Cyclic voltammetry (CV) curves (Fig. 4) were recorded as close as possible to the maximal current densities obtained during polarization (carbon cloth, day 20 in fig 1, $J = 38 \text{ A}/\text{m}^2$; SS foam, day 16 in Fig. 2B, $J = 82 \text{ A}/\text{m}^2$). Carbon cloth gave identical CVs to those previously reported for the same system. In particular, the maximum current plateau was reached from potentials around $-0.3 \text{ V}/\text{SCE}$ ²¹. The maximum current plateau was just multiplied by a factor of around 4 here due to use of acetate concentrations of 20 mM in the present work instead of 10 mM previously.

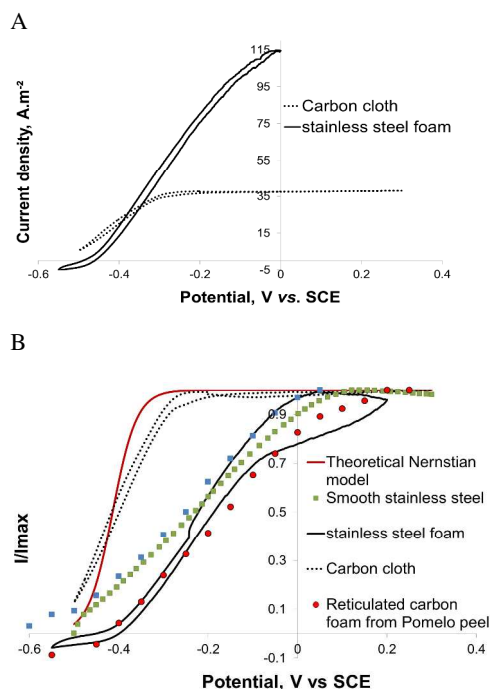


Fig 4: Cyclic voltammetry curves (1 mV/s) for carbon cloth and stainless steel foam bioanodes. A current density as a function of potential, B non-dimensional I/I_{max} as a function of potential. Three curves were reported from the literature for stainless steel plates¹⁰, carbon foam from Kenaf stem¹³ or Pomelo peel¹⁴.

CVs for SS foam bioanodes were stopped at 0.0 V to avoid possible disruption of the passive layer, which could lead to corrosion. Actually, 316 SS would not pose any corrosion problem in this zone of potential, but foams may be more sensitive to corrosion than the same SS grade plain material. Potential values have consequently been severely limited to 0.0 V/SCE to be sure not to induce corrosion of the foam. SS foam bioanodes showed less efficient electrochemical kinetics than

carbon cloth bioanodes (Fig. 4B). A larger overpotential was required for the current to start to increase and the maximum plateau was reached at around 0.05 V/ECS. The kinetics exhibited by the SS foam was similar to those already reported for SS plates¹⁰ and other carbon foams^{13,14}. It must be concluded that the carbon cloth used here possessed a fairly rare capability to ensure close-to-Nernstian electron transfer with wild electroactive biofilms. The SS foam had more conventional current-potential behaviour and the CV curves showed that it could provide up to 115 A/m² at +0.0 V/SCE. It consequently opens up an avenue for further improving SS foam bioanodes by working on the interfacial electron transfer with a view to pulling it up towards Nernstian-close kinetics. Work is now in progress to investigate the electron transfer kinetics and to identify the microbial communities on both carbon cloth and SS foam with this objective.

Experimental

Electrochemical experiments

Garden compost (EcoTerre) was mixed with water (1 kg in 1.5 L) containing 60 mM KCl under stirring for 24 h. The mix was then filtered through felt cloth and the leachate was used as medium after addition 20 mM of sodium acetate. The stainless steel foam AISI 316 (Fe/Cr18/Ni10/Mo3) was purchased from Goodfellow (Cambridge, UK; reference LS318529). The foam was 6.35 mm thick and presented 24 pores/cm. Carbon cloth was purchased from PaxiTech (Grenoble, France). The cloth electrode was composed of 10- μ m-diameter carbon fibers assembled into tightly woven 300- μ m-diameter threads. Microbial anodes were formed in 500-mL reactors, each equipped with a 2-cm² projected surface area working electrode connected electrically via a thin platinum wire. Working electrodes were polarized at -0.2 V with respect to a saturated calomel reference electrode (SCE, 0.245 V/SHE) in 3-electrode set-ups using a multi-channel potentiostat. Experiments were conducted at 40°C. Additions of 20 mM acetate were made when the current dropped to zero. Polarization was periodically suspended to perform cyclic voltammetry at 1 mV s⁻¹.

Scanning electron and Epifluorescence microscopies

Electrode materials were examined with a LEO 435 VP-Carl Zeiss SMT scanning electron microscope operating at 10 kV acceleration voltage and image acquisition used the LEO UIF software. Epifluorescent microscopy was performed by staining the bioanodes for 10 minutes in the dark with a 0.01% solution of orange acridine (A6014 Sigma). Bioanodes were then imaged with a Carl Zeiss AxioImager M2 microscope equipped for epifluorescence with an HBO 50 W ac mercury light source and the Zeiss 09 filter (excitor HP450–490, reflector FT 10, barrier filter LP520). Images were acquired with a monochrome digital camera (Evolution VF) every 0.5 μ m along the Z-axis and the set of images was processed with the Axiovision® software

Conclusion

SS foam is a very promising material for the design of microbial bioanodes. Its open structure favours the formation of biofilm,

with a large surface area exposed to the solution allowing current densities up to 82 A/m² at -0.2 V/SCE. This represents the highest value obtained with mono-layered microbial bioanodes to date. Current density of 115 A/m² was reached at 0.0 V/SCE. The electrochemical kinetics must now be improved with the view to generating such high current density at lower potential.

Acknowledgements

The authors thank the French National Research Agency (ANR) for financial support through the projects “Agri-Elec (ANR-008-BioE-001)” and “BioCathInox (ANR-11-JS09-016-01)”.

Notes and references

1. C. Dumas, R. Basséguy, and A. Bergel, *Electrochim. Acta*, 2008, **53**, 5235–5241.
2. C. Dumas, A. Mollica, D. Féron, R. Basséguy, L. Etcheverry, and A. Bergel, *Bioresour. Technol.*, 2008, **18**, 8887–8894.
3. L. Pons, M.-L. Delia, and A. Bergel, *Bioresour. Technol.*, 2011, **102**, 2678–2683.
4. L. Pons, M.-L. Delia, R. Basseguy, and A. Bergel, *Electrochim. Acta*, 2011, **56**, 2682–2688.
5. A. Bergel, D. Féron, and A. Mollica, *Electrochem. Commun.*, 2005, **7**, 900–904.
6. B. Erable, and A. Bergel, *Bioresour. Technol.*, 2009, **100**, 3302–3307.
7. C. Dumas, R. Basséguy, and A. Bergel, *Electrochim. Acta*, 2008, **53**, 2494–2500.
8. S. Chen, Y. Chen, G. He, S. He, U. Schröder, and H. Hou, *Biosens. Bioelectron.*, 2012, **34**, 282–285.
9. Y. Zhang, J. Sun, Y. Hu, S. Li, and Q. Xu, *Int. J. Hydrog. Energy*, 2012, **37**, 16935–16942.
10. D. Pocaznoi, A. Calmet, L. Etcheverry, B. Erable, and A. Bergel, *Energy Environ. Sci.*, 2012, **5**, 9645–9652.
11. S. Chen, H. Hou, F. Harnish, A. S. Patil, A. Carmona-Martinez, S. Argawal, Y. Zhang, S. Sinya-Ray, L. A. Yarin, A. Greiner, and U. Schröder, *Energy Environ. Sci.*, 2011, **4**, 1417–1421.
12. M. Zhou, M. Chi, J. Luo, H. He, and T. Jin, *J. Power Sources*, 2011, **196**, 4427–4435.
13. S. Chen, G. He, X. Hu, M. Xie, S. Wang, D. Zeng, H. Hou, and U. Schröder, *ChemSusChem.*, 2012, **5**, 1059–1063.
14. S. Chen, Q. Liu, G. He, Y. Zhou, M. Hanif, X. Peng, S. Wang and H. Hou, *J. Mater. Chem.*, 2012, **22**, 18609–18613.
15. R. Rousseau, X. Dominguez-Benetton, M.-L. Délia, and A. Bergel, *Electrochem. Commun.*, 2013, **33**, 1–4.
16. D. A. Finkelstein, L. M. Tender, and J. G. Zeikus, *Environ. Sci. Technol.*, 2006, **40**, 6990–6995.
17. S. Chen, G. He, Q. Liu, F. Harnish, Y. Zhou, Y. Chen, M. Hanif, S. Wang, X. Peng, H. Hou and U. Schröder, *Energy Environ. Sci.*, 2012, **5**, 9769–9772.
18. X. Liu, X. Du, X. Wang, N. Li, P. Xu, and Y. Ding, *Biosens. Bioelectron.*, 2013, **41**, 848–851.
19. X. Xie, M. Ye, L. Hu, N. Liu, J. R. McDonough, W. Chen, H. N. Alshareef, C. S. Criddle and Y. Cui, *Energy Environ. Sci.*, 2012, **5**, 5265–5270.
20. X. Zhang, M. Epifanio, and E. Marsili, *Electrochim. Acta*, 2013, **102**, 252–258.
21. B. Cercado, N. Byrne, M. Bertrand, D. Pocaznoi, M. Rimboud, W. Achouak, A. Bergel, *Bioresour. Technol.*, 2013, **134**, 276–284.